16th International Workshop on Water Waves and Floating Bodies
22.-25. April 2001, AKI Grand Hotel, Hiroshima

Influence of Canal Topography on Ship Waves in Shallow Water

Rupert Henn and Som D. Sharma
Institute of Ship Technology
Mercator University, Duisburg, Germany

Tao Jiang
VBD - European Development Centre for Inland and Coastal Navigation
Duisburg, Germany

1 INTRODUCTION

The waves generated by ships sailing on rivers or canals differ much from those in the open deep sea. Shallow water waves are typically steeper and, hence, nonlinear. They can damage river banks and endanger other ships. Natural rivers and artificial canals are getting increasingly too small for the present and future traffic. To survive in today's aggressive competition between different modes of transport inland ships have to become larger and faster. With increasing ship size the ratio of water depth to draft is getting smaller and, hence, fairways need to be dredged.
In this work the influence of the bottom topography of a canal on the waves generated by a ship at near-critical speed is studied. The wave pattern is found to differ significantly from the horizontal bottom case. Moreover, the danger arising from a ship sailing in a canal at an ill-adapted speed is pointed out. The calculations are based on shallow-water wave equations of the Boussinesq type, which have been previously used to successfully simulate the waves generated by a ship in a canal with a horizontal bottom, see Jiang & Henn (1999).

2 MATHEMATICAL FORMULATION

2.1 Coordinate System

A right-handed ship-bound coordinate system *Oxyz* is used. The origin *O* lies at the stern in the intersection of the undisturbed water-plane and the ship's longitudinal center-plane. The *x*-axis points in the direction of ship's forward motion; the *z*-axis, vertically upwards. The ship sails at speed *V* along the centerline of the canal. Running trim and sinkage are ignored.

2.2 Field equations

The fluid motion is described by the modified Boussinesq equations as given by Jiang (1998):

$$z_t - Vz_x + (z_x + h_x)u + (z + h)(u_x + v_y) + (z_y + h_y)v = 0$$

$$\begin{aligned} &u_t - Vu_x + uu_x + vu_y + gz_x \\ &-\frac{h}{2}[h_{xx}u_t + 2h_x u_{tx} + hu_{txx} + h_{xy}v_t + h_y v_{tx} + h_x v_{ty} + hv_{txy} \\ &\quad - V(h_{xx}u_x + 2h_x u_{xx} + h_{xy}v_x + h_y v_{xx} + h_x v_{xy})] \\ &-\frac{h^2}{3}[u_{xxt} + v_{xyt} - V(u_{xxx} + v_{xxy})] = 0 \end{aligned}$$

$$\begin{aligned} &v_t - Vv_x + uv_x + vv_y + gz_y \\ &-\frac{h}{2}[h_{xy}u_t + h_x u_{ty} + h_y u_{tx} + hu_{txy} + h_{yy}v_t + 2h_y v_{ty} + hv_{tyy} \\ &\quad - V(h_{xy}u_x + h_x u_{xy} + h_y u_{xx} + h_{yy}v_x + 2h_y v_{xy})] \\ &-\frac{h^2}{3}[u_{txy} + v_{tyy} - V(u_{xxy} + v_{xyy})] = 0 \end{aligned}$$

Here, $h(x,y)$ is the water depth, $\zeta(x,y,t)$ is the wave elevation, $u(x,y,t)$ and $v(x,y,t)$ are the depth-averaged perturbation velocity components in the x and y directions, respectively, t is the time, and g is the acceleration due to gravity.

2.3 Boundary conditions

On the boundaries of the computational domain sufficiently ahead of and behind the ship the Sommerfeld radiation condition

$$q_t + s q_x = 0$$

is applied, where q stands for each of the variables ζ, u and v, with $s = -V + \sqrt{gh}$ ahead of the ship and $s = -V - \sqrt{gh}$ behind the ship. The ship and canal are assumed to be both symmetric about their common longitudinal center-plane. So the entire flow is symmetric:

$$z(y) = z(-y),\ u(y) = u(-y),\ v(y) = -v(-y).$$

Therefore, the computational domain may be restricted to the half-plane $y \geq 0$. The vertical canal side-walls are supposed to be impermeable and perfectly reflecting.

2.4 Ship modeling

The flow perturbation caused by the ship hull is locally approximated by the slender-body theory. Therefore, the transverse velocity component v on the center-plane $y = +0$ is given by

$$v = \begin{cases} -\frac{1}{2}\frac{V}{h}\frac{\mathrm{d}S}{\mathrm{d}x} & ,\ 0 \leq x \leq L \\ 0 & ,\ \text{elsewhere} \end{cases}$$

An inland passenger ferry (Main dimensions: $L = 39.29$ m, $B = 8.84$ m and $T = 1.2$ m) is used as an exemplary ship; for further details see Jiang & Sharma (1998).

3 NUMERICAL METHOD

The field equations are discretized in space and time using the (symmetric) Crank-Nicolson finite difference scheme. The resulting sparse matrix is solved by a standard SOR (Successive Over-Relaxation) method, namely, the Gauss-Seidel algorithm. A detailed description can be found in Jiang (1998).

4 CANAL TOPOGRAPHY

Two essentially different types of canal-bottom topography are simulated: (i) A set of polygonal cross-sectional profiles which are uniform over the whole length of the canal; (ii) A rectangular profile with linearly decreasing water depth in the direction of ship's motion.

4.1 Configuration A

In configuration A the canal is 100 m wide; the water depth is 5 m in the central portion between two symmetric knuckle lines from where it decreases linearly to 1 m at the vertical side-walls. The y-coordinate of the knuckle varies from 50 m in case (a) – that is a rectangular profile – through 37.5 m (b), 25 m (c) to 12.5 m (d), see Fig. 1. Such profiles occur in many inland water canals.

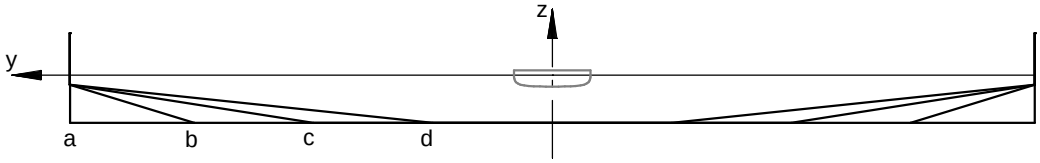

Fig. 1 Four different profiles of the canal configuration A

4.2 Configuration B

In configuration B the canal is also 100 m wide; the water depth varies from 5 m in the center to 3 m at the side walls as shown in Fig. 2, simulating a natural river with a deepened fairway.

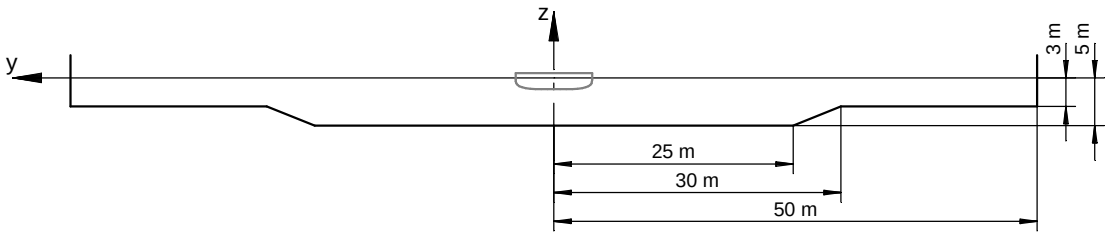

Fig. 2 Profile of the canal configuration B

5 RESULTS

5.1 Configuration A

Fig. 3 shows calculated wave patterns at ship speed 7 ms^{-1} corresponding to local depth Froude number unity. In other words, the ship is sailing at critical speed for the depth at the canal center. In the rectangular profile (a) solitary waves running ahead of the ship can be clearly observed. They vanish gradually as the shallower outer region of the profile gets larger: (b) → (c) → (d), probably because the Froude number based on mean depth grows increasingly supercritical.

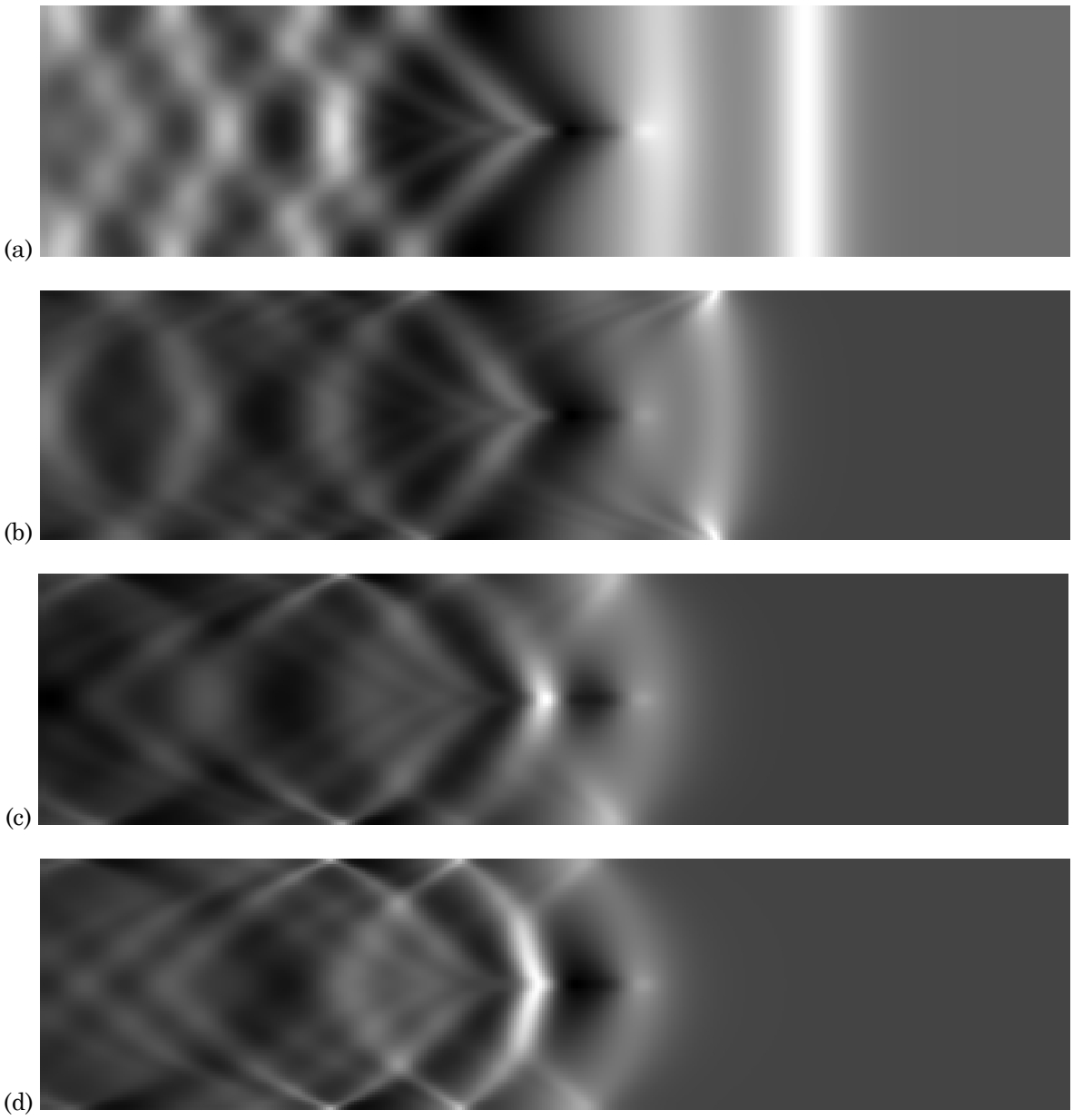

Fig. 3 Density plots of wave patterns at the same (locally critical) speed in different canal profiles

5.2 Configuration B

The ship moves again at a speed of 7 ms^{-1}. Fig. 4 shows the calculated wave pattern and longitudinal wave cuts at two chosen transverse locations. Looking first at the wave pattern, two solitary waves are evident. But whereas in the canal with a horizontal bottom (Fig. 3a) the amplitude of the solitary wave is constant over the full canal width, here the wave amplitude increases dramatically toward the side-walls. This may be hazardous for ambient traffic, specially for small craft that preferably sail in the outer shallower region of the canal to evade heavier vessels at the center. Comparing now the wave cut along the canal center-line (y = 0) with that near the side-wall (y = 41.6 m), it is seen that the maximum wave elevation in the latter is twice as high. Such high waves near the side-walls are, of course, also a menace to the river banks.

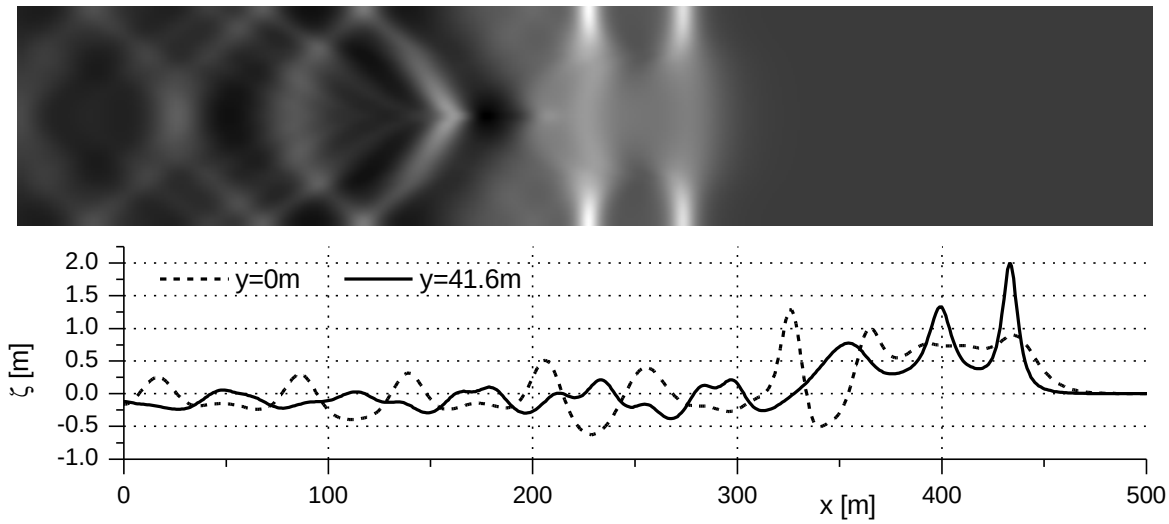

Fig. 4 Wave pattern and longitudinal wave-cuts at locally critical speed in a river-like canal

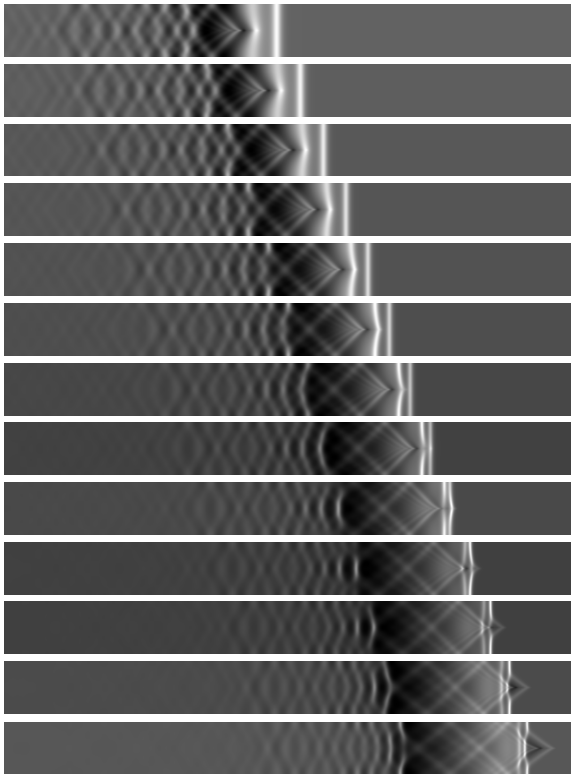

Fig. 5 Density plots of wave pattern generated by a ship moving onto a beach

5.3 Ship moving into a gradually shallower region

Fig. 5 shows a time series of density plots of the wave pattern produced by a ship sailing steadily into shallower water on the center-line of a rectangular canal with longitudinally sloping bottom. It is somewhat like running onto a beach. The ship starts its run in water of depth 5 m. Soon two solitary waves are generated. Before more solitary waves can be generated the water gets shallower. The second solitary wave being on deeper water is always faster and finally catches up with the first, while the ship overtakes them both. In the last plot in Fig. 5 the ship has reached the right edge of the calculation domain where the water is 1 m deep.

6 CONCLUSIONS

It has been shown that the bottom topography has an important influence on the waves generated by a ship in a shallow canal. The typical solitary waves generated by ships moving at near-critical speeds in shallow canals and easily observed in model tests acquire a more complex geometry if the canal bottom is uneven. The local depth Froude number is not the simple criterion for their occurrence. The specially high waves prevailing in the shallow bank zones of the canal may endanger other ships and damage the embankment. As a precaution ships must not sail at transcritical speeds in rivers and canals with river-like profiles.

Although wave resistance was not explicitly considered in this work, it is reasonable to expect that it will also be subject to the influence of bottom topography. It would be of much interest to model a more natural river bank as a partially reflecting boundary in future studies.

7 REFERENCES

Jiang, T.: Investigation of waves generated by ships in shallow water, Proc. 22nd Symposium on Naval Hydrodynamics, Washington D.C./USA, 1998

Jiang, T. & Sharma, S. D.: Wavemaking of flat ships at transcritical speeds, Proc. 19. Duisburger Kollqium Schiffstechnik/Meerestechnik, Duisburg 1998 (in german)

Jiang, T. & Henn, R.: Numerical investigation shallow-water wave equations of Boussinesq type, Proc. 14th Intl. Workshop on Water Waves and Floating Bodies, Port Huron/MI, USA 1999